Journal of proteome research

Article

pubs.acs.org/jpr

Mass Spectrometry Approach and ELISA Reveal the Effect of Codon Optimization on N-Linked Glycosylation of HIV-1 gp120

Kourosh Honarmand Ebrahimi,*[,†,§] Graham M. West,[‡,∥] and Ricardo Flefil[‡]

[†]Department of Infectious Diseases and [‡]Mass Spectrometry and Proteomics, The Scripps Research Institute, Scripps Florida, 130 Scripps Way No. 2A2, Jupiter, Florida 33458, United States,

[§]Department of Biotechnology, Delft University of Technology, Julianalaan 67, 2628BC Delft, The Netherlands

Supporting Information

ABSTRACT: The genes encoding many viral proteins such as HIV-1 envelope glycoprotein gp120 have a tendency for codons that are poorly used by the human genome. Why these codons are frequently present in the HIV genome is not known. The presence of these codons limits expression of HIV-1 gp120 for biochemical studies. The poor codons are replaced by synonymous codons that are frequently present in the highly expressed human genes to overexpress this protein. Whether this codon optimization affects functional properties of gp120 such as its N-linked glycosylation is unknown. We applied a bottom-up mass-spectrometry-based workflow for the direct measurement of deglycosylated and unglycosylated peptides with putative N-linked glycosylation sites, that is, NxS/T motifs. Using this mass-spectrometry approach in combination with ELISA, it is found that codon optimization significantly reduces the frequency with which the dolichol pyrophosphate-linked oligosaccharide is added by the catalytic subunits of oligosaccharide transferase complex to the glycosylation sites. This reduction affects binding of glycan-dependent broadly neutralizing antibodies. These data are essential for biochemical studies of gp120 and successful development of a vaccine against HIV-1. Furthermore, they demonstrate a mass-spectrometry approach for studying the site-specific N-linked glycosylation efficiency of glycoproteins.

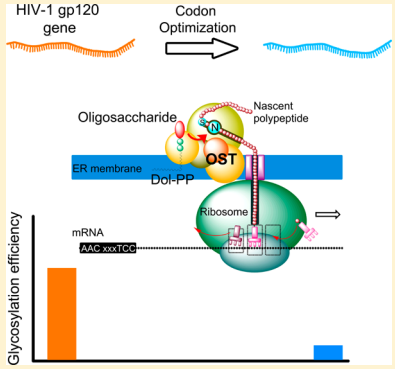

KEYWORDS: *HIV-1, envelope glycoprotein, glycosylation, codon optimization, gp-120*

INTRODUCTION

HIV-1 genome has several codons that are poorly used by the human genome (poor codons) and that limit expression of viral proteins such as HIV-1 envelope glycoprotein gp120.[1] It is not known why the HIV-1 genome has evolved to contain these poor codons. To overexpress gp120 for biochemical[2,3] and vaccine research studies,[4−7] the gene encoding this protein has been codon-optimized: poor codons are replaced by the synonymous codons that are frequently present in the highly expressed human genes. Whether codon optimization affects functional properties of gp120 such as its N-linked glycosylation is unknown.

Several putative N-linked glycosylation sites, that is, NxS/T motifs, are present in gp120. The addition of oligosaccharides to these sites leads to the formation of a glycan shield that protects the protein backbone from antibody recognition and facilitates HIV-1 escape from the immune system.[8] Therefore, efficient glycosylation of these sites is essential for HIV-1 infectivity. The efficiency with which the asparagine residue of the NxS/T motifs is glycosylated by the oligosaccharide transferase (OST) complex is dependent on whether S or T is present after amino acid at position x,[9] the amino acid that occupies position x,[10] and the amino acid after the NxS/T motif.[11] Determining the glycosylation efficiency of each NxS/T motif in gp120 and understanding the factors that change this efficiency will provide new insights into the mechanism by which some HIV-1 isolates may escape from the newly identified glycan-dependent broadly neutralizing antibodies (bNABs) such as PG9 and PG16[12,13] or PGT128.[14] These data are essential for successful design of a vaccine against HIV-1.

In the present study, we have applied a new mass spectrometry workflow in combination with ELISA experiments to study the effect of synonymous codon usage on the glycosylation efficiency of the NxS/T motifs in HIV-1 gp120. The novelty of our workflow is based on the deglycosylation of gp120 by PNGase F activity[15] that cleaves oligosaccharides from the NxS/T sequence and deamidates the asparagine residue to form the DxS/T sequence, which can be measured by mass spectrometry. We show that codon optimization of gp120 reduces the frequency with which the catalytic subunits of OST complex, that is, STT3A and STT3B,[16,17] add the dolichol pyrophosphate-linked oligosaccharide to the asparagine residue of the NxS/T motifs. Thus, it appears that the presence of poor codons, which limit the gp120 expression, assures efficient glycosylation of the asparagine residue of the NxS/T sequences of gp120.

Received: July 16, 2014
Published: September 25, 2014

   dx.doi.org/10.1021/pr500740n | J. Proteome Res. 2014, 13, 5801−5811

EXPERIMENTAL PROCEDURE

Expression and Purification of WC-gp120 or CO-gp120

HEK293T cells were used for expression of different constructs of gp120. Cells were grown on cell culture flasks with a surface area of 175 cm^3. gp120 was from HIV-1 ADA isolate. For expression of wild-type codon gp120 (WC-gp120), to each flask 24 μg of plasmid containing the gene encoding WC-gp120 plus 6 μg of plasmid containing the gene encoding HIV-1 rev and 6 μg of plasmid containing the gene encoding HIV-1 tat was added to transfect the cells. Transfection was performed using calcium phosphate transfection kit (Clontech). Eight hours post-transfection the medium was replaced by fetal-bovine-serum (FBS)-free medium, and after 72 h cell-free supernatant was collected. The subsequent steps for gp120 purification were performed on ice unless otherwise stated. This was to minimize possible autodiamidation (background deamidation) of asparagine residues[18] that were not glycosylated. Autodeamidation of asparagine residues in peptides occurs very slowly (half-life is between 10 to 90 days at 37 °C depending on the neighboring sequence of asparagine).[18] Because gp120 has several putative glycosylation sites and many of these sites contain high-mannose oligosaccharides,[19] gp120 was purified using agarose-conjugated lectin from *Galanthus nivalis* (snowdrop) (Sigma-Aldrich). This lectin has specificity for terminal high mannose residues such as those that contain Man(α1−3) Man.[20] To capture gp120 from the supernatant, 1 mL of agarose-conjugated lectin from *Galanthus nivalis* was added per 200 mL of supernatant, and the solution was incubated overnight at 4 °C. The next day, the solution was run through an Econo-Pac column (BioRad). Agarose-conjugated lectin beads were captured in the column and were washed using 30 mL of 0.65 M NaCl phosphate buffer saline (PBS) and 20 mL of PBS. Subsequently, to dissociate gp120 from lectin, we added 6 mL of 1 M methyl-α-D mannopyranoside (in PBS) to the beads, and the column was incubated at 4 °C for 1 to 2 h. Then, the flow-through that contained gp120 was collected and was subjected to overnight dialysis against the PBS buffer. Using *Galanthus nivalis* lectin efficient purification of gp120 was achieved (Figure S1 in the Supporting Information). Protein concentration was measured with the Pierce 660 protein assay (Thermo scientific). For expression of codon optimized gp120 (CO-gp120) and its mutants, 293T cells were transfected with 24 μg plasmid (unless otherwise mentioned) containing the gene encoding CO-gp120 or its mutants. Subsequent steps were exactly the same as those described above for expression and purification of WC-gp120. CO-gp120 and WC-g120 were expressed in parallel using the same stock of HEK293T cells and identical cell growth conditions. Furthermore, protein purification was performed at the same time using one lectin batch and the same reagents.

Expression and Purification of CD4-Ig

HEK293T cells were used for expression of CD4-Ig. 293T cells were transfected with 24 μg plasmid containing the gene encoding CD4-Ig. 8 h post-transfection the medium was replaced by FBS free medium, and after 72 h cell-free supernatant was collected. One mL of protein A beads (Sigma-Aldrich) was added to 200 mL of supernatant, and the solution was incubated overnight at 4 °C. Next day, the solution was run through an Econo-Pac column (BioRad) to capture the beads. Thirty mL of 0.65 M NaCl PBS and 20 mL of PBS was used to wash the beads. Subsequently, 6 mL of 5 M $CaCl_2$ (in PBS) was added to dissociate CD4-Ig from protein A beads. Then, the flow-through, which contained CD4-Ig, was collected and was subjected to overnight dialysis against the working PBS buffer. Protein concentration was determined using the Pierce 660 protein assay (Thermo Scientific).

PNGase F Treatment and SDS-Gel Electrophoresis

PNGase F kit (New England Biolabs) was used to remove oligosaccharides from gp120.[21] The protein samples were first denatured according to the manufacturer protocol. Subsequently, PNGase F enzyme was added, and the reactions were incubated at 37 °C for at least 12 h.

Site-Directed Mutagenesis

Five constructs were prepared to change the codons downstream of the glycosylation site N156 in the codon-optimized gp120 (CO-gp120). In each construct five codons were changed: codons 26−30 in construct Z1 (Z1-CO-gp120), codons 31−35 in construct Z2 (Z2-CO-gp120), codons 36−40 in construct Z3 (Z3-CO-gp120), codons 41−45 in construct Z4 (Z4-CO-gp120), and codons 46−50 in construct Z5 (Z5-CO-gp120). For simplicity of mutagenesis studies, we decided to change five codons at a time. Site-directed mutagenesis was used to change the codons to those of synonymous codons present in the gene encoding WC-gp120 and to perform S158T or T162S mutations. The forward primers were: Z1-CO-gp120, 5′ CTACCGCCTGGACGTAGTACCAATAGATAACGACAACACCAGC 3′; Z2-CO-gp120, 5′ GGTGCCATCGACAATGATAATACTAGCTACCGCCTGATC 3′; Z3-CO-gp120, 5′ CGACAACACCAGCTATAGGTTGATAAATTGCAACACCAGC 3′; Z4-CO-gp120, 5′ CGCCTGATCAACTGTAATACCTCAACCATCACCCAGGCATG 3′; Z5-CO-gp120, 5′ CAACACCAGCACCATTACACAGGCCTGTCCCAAGGTGAGC 3′; S158T-CO-gp120, 5′ GAGATCAAGAACTGCACCTTCAACATCACCAC 3′; and T162S-CO-gp120, 5′ CAGCTTCAACATCAGCACCAGCATCCGCG 3′.

The reverse primers were complementary to the forward primers. Site-directed mutagenesis was performed using a quick-change site-directed mutagenesis kit (Alginet). The presence of desired mutations was confirmed by sequencing (Genewiz).

Proteomic Gel Band Digest and MS/MS Analysis

Gel bands were dehydrated using a 2:1 acetonitrile/25 mM ammonium bicarbonate solution. This was followed by two times wash using a 25 mM ammonium bicarbonate solution. The existing disulfide bonds were reduced by the addition of 10 mM DTT solution and incubation at 56 °C for 1 h. The resulting thiols were alkylated with 55 mM iodoacetamide (IDA) in the dark for 45 min. Proteins were digested using 35 mL of a 12.5 ng/mL solution of trypsin (Promega − V5111) in 25 mM ammonium bicarbonate overnight at 37 °C. Dried peptides were brought up in 23 μL of 0.1% formic acid and sonicated for 5 min at RT in a Branson 5510 sonicator. 10 μL of sample was injected on column for LC−MS analysis. The samples were run on either a linear trap/Orbitrap or a quadrupole/Orbitrap. The linear trap/Orbitrap consisted of an Eksigent nano LC-as-2 autosampler/nano LC ultra ID plus loading pump coupled to a nano ESI source (Proxeon, Odense, Denmark) on a Finnigan LTQ Orbitrap (Thermo Scientific). The quadrupole/Orbitrap consisted of an Easy-nLC 1000 coupled to a Nanospray Flex ion source with a Q Exactive (Thermo Scientific). All columns were self-packed capillaries. Trap columns (IntegraFrit IF360-100-50-N-5) were used to desalt samples in-line with LC using a T-junction. Trap

dx.doi.org/10.1021/pr500740n | J. Proteome Res. 2014, 13, 5801−5811

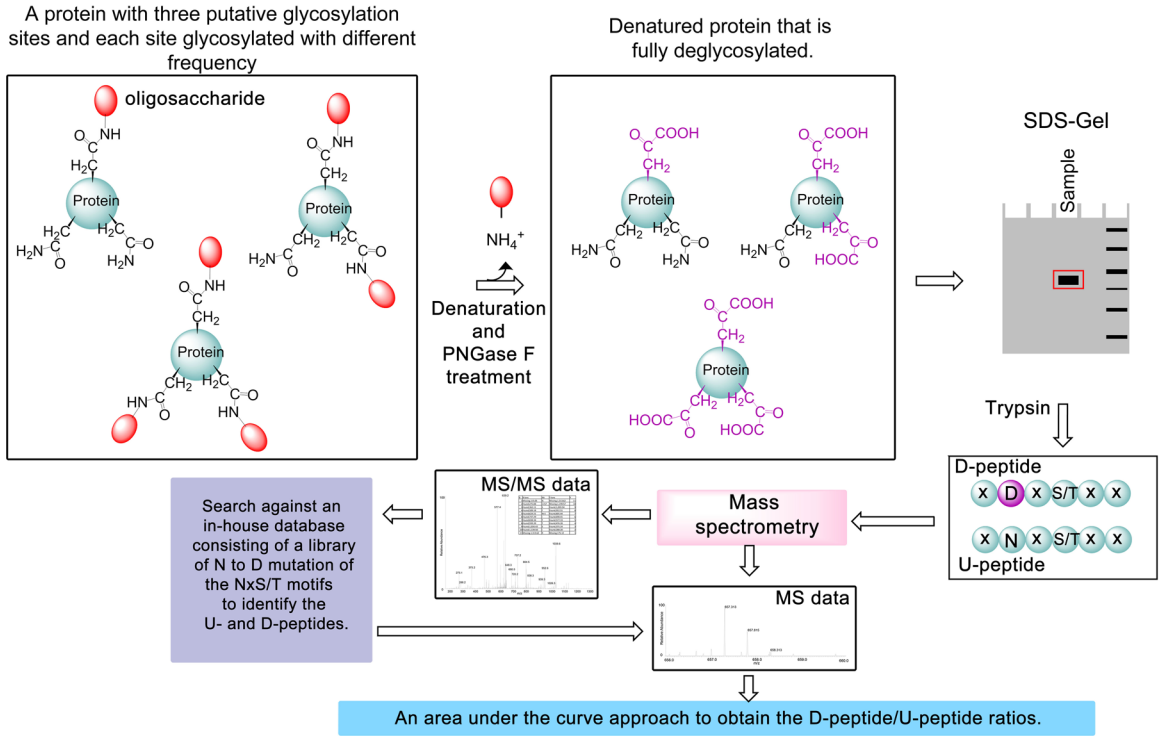

Figure 1. Mass spectrometry approach to measure the frequency with which a putative N-liked glycosylation site is glycosylated. A glycoprotein that has three putative glycosylation sites is shown. In the purified glycoprotein each glycosylation site exists either as glycosylated or as unglycosylated. After purification of the glycoprotein it is treated with PNGase F. This enzyme removes the N-linked olicosaccharide from the NxS/T motif in the glycosylated sites and converts the NxS/T motif to the DxS/T motif. After PNGase digestion a fraction of protein contains deglycosylated sites (purple) and a fraction has unglycosylated sites (black). The protein sample is run onto an SDS-gel and the protein band is excised. Subsequently, trypsin digestion leads to the formation of peptides in which the NxS/T motif was deglycosylated by PNGase F activity (D-peptide) and of peptides in which the NxS/T motif was unglycosylated and was not affected by PNGase F activity (U-peptide). D-peptide has a DxS/T motif and U-peptide has an NxS/T motif. Tryptic peptides are measured and identified by mass spectrometry. U and D peptides are identified by searching the MS/MS data against a database consisting of a library of N → D mutation of the NxS/T motifs. Finally, using the MS data of the identified D- and U-peptides and an area under the curve approach the relative D-peptide/U-peptide ratio is determined.

columns were packed with 2 cm stationary phase, and analytical columns (Cat# IntegraFrit IF360-75-50-N-5) were packed with 15 cm of stationary phase, Jupiter 4 μ Proteo 90A (04A-4396). LC gradients ran from 5 to 35% acetonitrile/0.1% formic acid over 60 min. For the LTQ, samples were analyzed using an *N*th-order double-play data-dependent acquisition (DDA) method sampling the top five most intense precursor ions at a resolution of 60 000. For the Q Exactive, samples were analyzed using a FullMS/dd-MS2 (Top10) method at a resolution of 70 000. The raw data were processed using Mascot Daemon v2.4.0 (Matrix Sciences) and searched against an in-house gp120 database. The gp120 in-house database contained N → D mutation in all of the NxS/T motifs plus S158T and T162S substitutions (Supporting Information). To determine the autodeamidation (background deamidation) of asparagine residues that were not in the NxS/T motif, we searched the raw data against an in-house database consisting a library in which all asparagine residues were mutated to D. Carbamidomethyl (Cys) was included as a fixed modification. Oxidation (Met), phosphorylation (Ser and Thr), and deamidation (Asn) were included as variable modifications. Enzyme specificity was set to trypsin. Mass accuracy was set to 10 ppm for precursor and 0.8 Da (20 mmu for Q Exactive) for product ions. The results from the database searches were imported into Scaffold v4.3.0, and identification parameters were set to 20% protein threshold, 1 peptide minimum, and 90% peptide threshold.

ELISA Experiments

Twenty-five μL of 2 mg/mL gp120 was added to the wells (except the wells in the first row) of each ELISA plate. To the first row of each plate 25 μL of buffer was added as blank. The plates were incubated at 37 °C for 2 h to coat the wells with gp120. Subsequently, gp120 or buffer was removed, and the wells were washed four times with 150 μL of 1×-DPBS-Tween 20 (0.05%) and two times with 150 μL of 1×-DPBS. Then, 150 μL of 1×-DPBS-5% milk was added and the plates were incubated at 37 °C for 2 h to block the wells. This was followed by the removal of the 1×-DPBS-5% milk and washing six times with 150 μL of 1×-DPBS-Tween 20 (0.05%) and two times with 150 μL of 1×-DPBS. Then, 50 μL of 10 mg/mL PG9 or CD4-Ig was added, and after 3 h of incubation at 37 °C, the wells were washed using 1×-DPBS-Tween 20 (0.05%) (eight times) and 150 μL of 1×-DPBS (two times). Finally, 50 μL of goat antihuman IgG, HRP-conjugated (1 μL in 5000 μL of 1×-DPBS-5% milk) was added, and plates were incubated at 37 °C for 1 h. The excess goat antihuman IgG was removed by washing the wells 10 times with 150 μL of 1×-DPBS-Tween 20 (0.05%) and two times with 150 μL of 1×-DPBS. Finally, 50 μL of 3,3′,5,5′-tetramethylbenzidine (TMB) was added. The reaction was incubated at room temperature until development of blue color. The reaction was stopped by the addition of TMB stop solution (pierce). UV−visible absorbance was recorded at 450 nm on a Victor3 V (PerkinElmer Life Sciences).

dx.doi.org/10.1021/pr500740n | *J. Proteome Res.* 2014, 13, 5801−5811

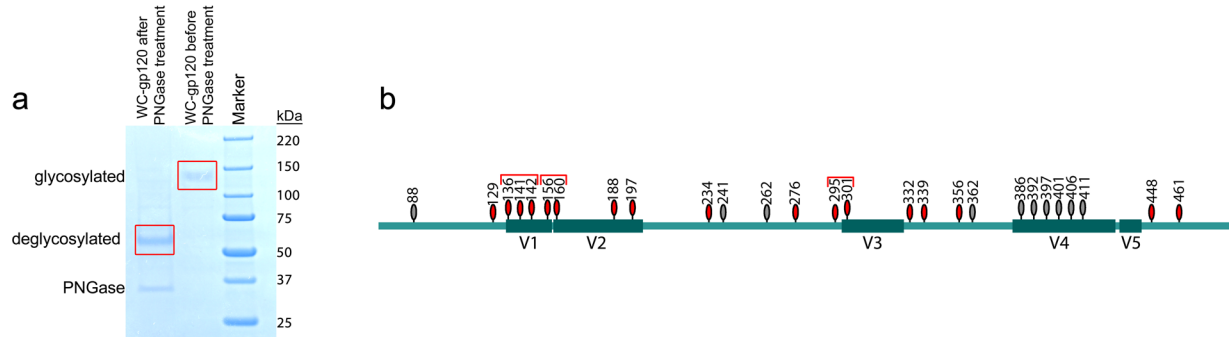

Figure 2. Identification of the glycosylation sites of HIV-1 gp120 using mass spectrometry. (a) SDS-gel electrophoresis of WC-gp120 before and after treatment with PNGase F. After treatment with PNGase F a band at 53 kDa appeared that corresponds to the polypeptide backbone of gp120, which does not have any oligosaccharide attached. (b) Glycosylation sites on gp120 for which D-peptides and U-peptides were identified are shown in red. The sites for which no peptide was identified are shown in gray; these sites were located on peptides with more than 35 amino acid residue. The glycosylation sites that are marked by a red bracket are located on one tryptic peptide.

RESULTS

Mass Spectrometry Approach to Study Site-Specific Glycosylation Efficiency

To measure the glycosylation efficiency of the asparagine residue (N) of the NxS/T motifs, we applied a simple mass spectrometry workflow (Figure 1). Each putative glycosylation site of a glycoprotein is glycosylated with a different frequency, and thus it exists either as glycosylated or as unglycosylated. A purified glycoprotein is a mixture of these forms (Figure 1). The N-linked oligosaccharides are removed by PNGase F treatment. PNGase F catalyzes the cleavage of N-linked oligosaccharides and it deamidates and hydrolyzes the asparagine side chain, thus effectively converting asparagine (N) to aspartic acid (D).[15,22,23] As a result, a fraction of protein contains the deglycosylated sites, that is, DxS/T sequence, and a fraction of protein contains unglycosylated sites, that is, NxS/T sequence (Figure 1). This deglycosylated protein sample is loaded onto an SDS-gel electrophoresis. Subsequently, the SDS-gel protein band is excised and digested using trypsin.[24] As a result, for each tryptic peptide with a putative glycosylation site two sequences are possible: (I) If asparagine was glycosylated the PNGase F treatment converted the NxS/T motif to DxS/T motif, deglycosylated peptide (D-peptide), and (II) if the asparagine was not glycosylated the PNGase F treatment did not alter the sequence in the NxS/T motif, unglycosylated peptide (U-peptide) (Figure 1). The tryptic peptides can then be sequenced and identified by mass spectrometry. The MS/MS data are searched against an in-house database consisting a library of N → D mutation of any NxS/T motif present to identify the D- and the U-peptides. After identification of the peptides, because the D-peptide is one Dalton heavier than its corresponding U-peptide, the D-peptide/U-peptide ratio, which represents the ratio of glycosylated over unglycosylated peptides, is obtained from the intact MS data using an area under the curve approach.

Mass Spectrometry Led to Identification of D- and U-Peptides

The mass spectrometry workflow shown in Figure 1 was used to identify the N-linked glycosylation sites of gp120 that were glycosylated and were included in our proteomic sequence coverage. The protein product of a gp120 gene that was not codon optimized, wild-type codon gp120 (WC-gp120), was used. After purification of WC-gp120, the protein was subjected to PNGase F digestion. A sample of the protein before addition of PNGase F and a sample after PNGase F treatment were loaded onto the SDS-gel to determine the efficiency of deglycosylation using PNGase F. Figure 2a shows that digestion with PNGase F effectively removed all of the N-linked oligosaccharides from gp120 and resulted a protein band with a molecular weight of ca. 53 kDa, which is equal to that of gp120 protein backbone with no oligosaccharide attached. Subsequently, the deglycosylated protein band was excised and was subjected to trypsin digestion and mass spectrometry analysis, as explained in Figure 1. A list of all peptides that were identified (i.e., Mascot scores >20) (Figure S2 and S3 in the Supporting Information) from a Mascot search against the database of N → D mutation of NxS/T motifs is given in the Supporting Information (Table S1). Our proteomic sequence coverage was >70% of gp120 amino acid sequence, and it included >60% of the putative glycosylation sites (Figure 2b). For all of these glycosylation sites both the deglycosylated peptide (D-peptide) and the unglycosylated peptide (U-peptide) were identified (Table S1 in the Supporting Information). The D-peptide/U-peptide ratio for these peptides was more than four (Table S2 in the Supporting Information). The glycosylation sites that were not identified were located on peptides with more than 35 amino acid residues (Figure S4 in the Supporting Information), and thus their identification requires digestion with an alternative protease.

Codon Optimization Reduces the Glycosylation Frequency of the NxS/T Motifs

Next, we applied our mass spectrometry approach to study the effect of codon optimization on the overall glycosylation efficiency of gp120 and on the glycosylation efficiency of individual NxS/T motifs. To this goal the glycosylation efficiency of the NxS/T motifs for WC-gp120 was compared with that of the NxS/T motifs for the gp120 protein product of the codon-optimized gene (CO-gp120) (Figure 3). The CO-gp120 was expressed at three different levels by adjusting the amount of plasmid that was used for the transfection of cells (Table 1): high expression (H-CO-gp120), medium expression (M-CO-gp120), and low expression (L-CO-gp120). The purified proteins were run onto a reducing SDS gel. We observed that the protein band of WC-gp120 was different than those of CO-gp120 expressed at three different levels (Figure 3a). We hypothesized that this difference was due to the difference in the frequency with which N-linked glycosylation sites were glycosylated. To check this we obtained the D-

dx.doi.org/10.1021/pr500740n | J. Proteome Res. 2014, 13, 5801−5811

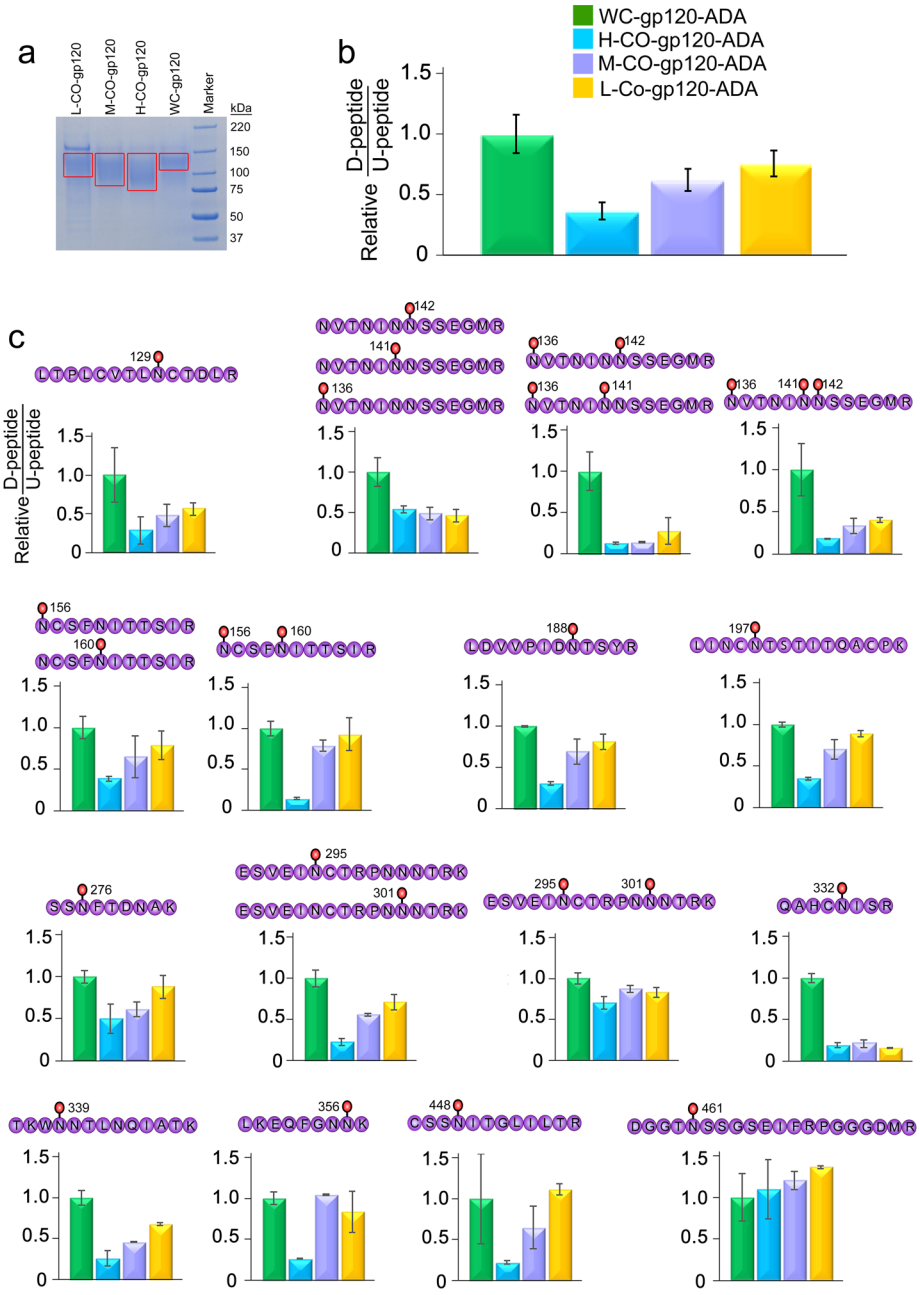

Figure 3. Codon optimization reduces the frequency with which each glycosylation site of gp120 is glycosylated. (a) SDS-gel electrophoresis of purified WC-gp120, H-CO-gp120, M-CO-gp120, and L-CO-gp120. (b) Results of mass spectrometry for the overall glycosylation efficiency of WC-gp120 and CO-gp120 expressed at three different levels. The histogram shows the sum of D-peptide/U-peptide ratios of all glycosylation sites. The D-peptide/U-peptide ratio for WC-gp120 was used as standard. (c) Results of mass spectrometry for the frequency with which each NxS/T motif was glycosylated. The D-peptide/U-peptide ratios for WC-gp120 were used as standard. For each peptide the D-peptide/U-peptide ratio for H-CO-gp120, M-CO-gp120, and for L-CO-gp120 was compared to that of standard (WC-gp120). The glycosylated peptides, which are shown on the top of each histogram, represent the D-peptides that were found by mass spectrometry. For the peptides with multiple glycosylation sites, namely, peptide with N136, N141, and N142, peptide with N156 and N160, and peptide with N295 and N301, different D-peptides are shown. For the peptides that had one peak in the MS, one histogram was plotted. Two different batches of proteins were tested, and for each batch experiments were repeated two times. The data are the average of these independent measurements ± standard deviation. Concentration of protein for each experiment was between 0.5 and 2 mg. All protein samples were expressed and purified in parallel under identical conditions.

peptide/U-peptide ratios for the peptides with NxS/T motifs (Figure 3b,c). D-peptide/U-peptide ratios for WC-gp120 were used as standard and the D-peptide/U-peptide ratios for H-CO-gp120, M-CO-gp120, and L-CO-gp120 were plotted relative to standard. This way we did not need to create standard curves with pure D- and U-peptides, and we were able to directly observe the decrease or increase in the D-peptide/U-peptide ratios for CO-gp120 compared with those for WC-gp120. A histogram of the sum of the D-peptide/U-peptide ratios for all of the NxS/T motifs (Figure 3b) showed that codon optimization reduced the overall glycosylation efficiency of gp120. This is consistent with the results of SDS-gel electrophoresis (Figure 3a). Subsequently, we plotted the D-peptide/U-peptide ratio of each peptide with one or more

dx.doi.org/10.1021/pr500740n | J. Proteome Res. 2014, 13, 5801−5811

Table 1. WC-gp120 and CO-gp120 Expression[a]

sample	μg gp120 plasmid	μg pcDNA empty vector	μg protein after purification
WC-gp120	24		24.2
H-CO-gp120	24		109.4
M-CO-gp120	1.2	22.8	48.5
L-CO-gp120	0.24	23.76	15.0

[a]CO-gp120 was expressed at three different levels by adjusting the amount of plasmid that was added to transfect cells: high expression (H-CO-gp120), medium expression (M-CO-gp120), and low expression (L-CO-gp120). For H-CO-gp120, the amount of CO-gp120 plasmid used for the transfection was equal to that of WC-gp120 plasmid used for the transfection. For M-CO-gp120 and L-CO-gp120 the amount of CO-gp120 plasmid used for the transfection was, respectively, 50- and 100-fold less than that used for H-CO-gp120. In the case of M-CO-gp120 and L-CO-gp120 the total amount of plasmid used for the transfection was set to 24 μg by adding an empty vector, that is, pcDNA.

Table 2. Non-Enzymatic Deamidation of Asparagine Residues Is Negligible[a]

Sequence	Auto-deamidated/non-deamidated peptides ratio	
	WC-gp120	H-CO-gp120
IKQIINMWQEVGK	0.08 ± 0.02	0.07 ± 0.03
NIIVQLK	0.04 ± 0.01	0.04 ± 0.01

[a]Two peptides are shown that contain one asparagine residue but no NxS/T motif. For these peptides nonenzymatic deamidation of asparagine led to formation of aspartate (D). The autodeamidated/nondeamidated peptides ratio for these peptides represents the approximate level of background deamidation.

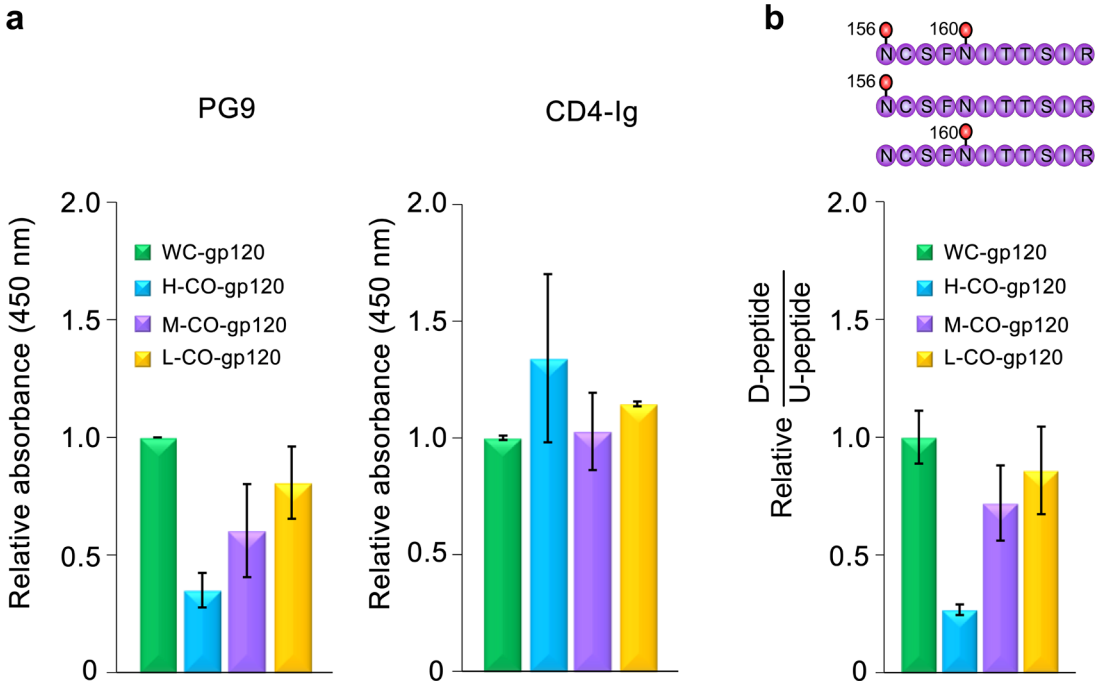

Figure 4. ELISA experiments confirmed the results of mass spectrometry. (a) PG9 and CD4-Ig binding to WC-gp120, H-CO-gp120, M-CO-gp120, and L-CO-gp120. The results of PG9 binding to WC-gp120 were used as standard. The results show that PG9 binding to CO-gp120 was decreased compared with WC-g120. The UV−visible absorbance was measured at 450 nm. The same batches of protein as those used for experiments in Figure 3b were used, and with each batch three independent measurements were performed. The data represent the average of these measurements ± standard deviation. The data for PG9 binding are corrected for small variations in concentration using the control experiment with CD4-Ig.Concentration of gp120 was 2 mg/mL and those of PG9 and CD4-Ig were 10 mg/mL. (b) Histogram showing the effect of codon optimization on glycosylation efficiency of N156 and N160 as measured by mass spectrometry. The histogram is obtained from the results of two histograms in Figure 3c: the histogram for the two peptides in which either N156 or N160 was glycosylated and the histogram for the peptide in which both N156 and N160 were glycosylated. These peptides are shown on the top of the histogram.

glycosylation sites (Figure 3c). For the peptides that have one NxS/T motif only one D-peptide/U-peptide ratio was obtained. For the peptides that have more than one NxS/T motif, different D-peptide/U-peptide ratios were obtained based on the number of the NxS/T motifs that were glycosylated and could be deglycosylated by PNGase F activity (Table S1 in the Supporting Information). For example, for the peptide with glycosylation sites N156 and N160, two D-peptide/U-peptide ratios were calculated (Figure 3c): one for two peptides in which either N156 or N160 was glycosylated

dx.doi.org/10.1021/pr500740n | J. Proteome Res. 2014, 13, 5801−5811

and which have one peak in the MS data and one for the peptide in which both N156 and N160 were glycosylated. The results for H-CO-gp120 showed that overexpression of gp120 reduced the glycosylation efficiency of all NxS/T motifs in CO-gp120 (Figure 3c). For most sites decreasing the expression level of CO-gp120 to a level less than that of WC-gp120, that is, L-CO-gp120, improved glycosylation efficiency of CO-gp120 but did not lead to full recovery compared to WC-gp120 (Figure 3c and Table 1).

Autodeamidation of Asparagine Residues Is Negligible

Our mass spectrometry workflow is based on PNGase F activity that removes oligosaccharides from the glycosylated NxS/T motifs and deamidates the asparagine (N) residue to form D-peptides (Figure 1). The fraction of unglycosylated NxS/T motifs, which was counted as the fraction of U-peptide, was not deamidated by PNGase F activity but might be deamidated nonenzymatically (autodeamidation).[25−27] Therefore, we checked if nonenzymatic deamidation might have affected the results in Figure 3b,c. To this goal, we used mass spectrometry to detect nonenzymatic deamidation of asparagine residues that were not in the NxS/T motif. We searched the MS/MS data for WC-gp120 and CO-gp120 against an in-house database consisting of a gp120 library in which all asparagine residues were mutated to aspartate. Our proteomic sequence coverage included 15 asparagine residues that are not in the NxS/T sequence (Figure S4 in the Supporting Information). These asparagine residues are not glycosylated and will not be deamidated by PNGase F activity, and their deamidation can only occur nonenzymatically. Thus, the level of the nonenzymatic deamidation of these residues can be considered as the level of background deamidation. Eight of these asparagine residues were found to be autodeamidated (Table S3 in the Supporting Information). We chose two peptides, which have one asparagine residue but no NxS/T motif, and we determined the ratio of deamidated peptide to nondeamidated peptide (Table 2). The deamidated/nondeamidated peptides ratio for each WC-gp120 peptide was within experimental error identical to that of CO-gp120 peptide. Therefore, the differences between WC-gp120 and CO-gp120 in Figure 3 could not be due to autodeamidation of unglycosylated NxS/T motifs. Furthermore, comparison of the background deamidation level (Table 2) with the D-peptide/U-peptide ratio of the peptides with the NxS/T motif (Table S2 in the Supporting Information) suggested that nonenzymatic deamidation was negligible. Therefore, the D-peptide/U-peptide ratios could be considered equivalent to the glycosylated/unglycosylated peptides ratio and is a measure of the glycosylation efficiency.

ELISA Confirms the Results of Mass Spectrometry

Next, we used ELISA and we measured binding of PG9 to gp120 to test the results of mass spectrometry. PG9 is a glycan-dependent bNAB, and it recognizes oligosaccharides at positions N156 and N160,[13,28] which are located on a single tryptic peptide (Figure 3c). We measured PG9 binding to WC-gp120, H-CO-gp120, M-CO-gp120, and to L-CO-gp120 using ELISA (Figure 4a). The results for WC-gp120 were used as standard. As a control for PG9 binding we recorded CD4-Ig binding in parallel (Figure 4a). The control experiment using CD4-Ig was performed to test if CD4-Ig could properly bind all protein samples and to correct for possible small variations in the protein concentration among the wells. The results of CD4-Ig binding showed that the CD4 binding region of gp120 was not affected by codon optimization. PG9 binding to H-CO-gp120 was much less than that to WC-gp120, and the binding to CO-gp120 was increased as the overall CO-gp120 expression level was decreased (Figure 4a and Table 1). To directly compare the results of ELISA experiments with those of mass spectrometry we plotted a histogram that is obtained from the sum of the data for two histograms in Figure 3c: the histogram for two peptides in which either N156 or N160 was glycosylated and the histogram for the peptide in which both N156 and N160 were glycosylated. The results for PG9 binding measured by ELISA (Figure 4a) and the results for D-peptide/U-peptide ratio obtained by mass spectrometry (Figure 4b) were the same. Because with ELISA binding of PG9 to oligosaccharides was measured independent of the autodeamidation of unglycosylated asparagine residues, we concluded that the effect of background deamidation on the results of mass spectrometry was negligible.

Codons Downstream of N156 Affect PG9 Binding

In an attempt to check the effect of codon optimization on specific N-linked glycosylation sites, which are the target of glycan dependent bNABs, the effect of synonymous codon change at downstream of glycosylation sites N156 and N160 was tested. These sites were chosen because antibodies such as PG9 or PG16 that specifically bind to the oligosaccharides at these sites are very well characterized,[12,13,28−32] and thus we could use ELISA in combination with mass spectrometry. The distance between the translation site on ribosome and the site where oligosaccharide precursor is added by the catalytic subunits of OST complex to the NxS/T motif in a nascent polypeptide is proposed to be 30−50 amino acids.[33] Therefore, we hypothesized that a region between 25 and 50 codons downstream of the N156 codon might affect glycosylation efficiency or antibody binding (Figure 5a). To test this hypothesis, we divided this region to five subregions each consisting of five codons (15 nucleotides). In each subregion the optimized codons in the construct for expression of CO-gp120 were replaced by the poorly used synonymous codons that are present in the gene encoding WC-gp120. As a control we created two other mutants: S158T and T162S. These mutants were prepared because it is known that the NxT motif is glycosylated more efficiently than the NxS motif.[34] Therefore, S158T mutation is expected to increase the glycosylation efficiency at N156, and T162S mutation is expected to reduce the glycosylation efficiency at N160. The glycosylation efficiency of N156 and N160 in these constructs was studied using mass spectrometry (Figure 5b) and ELISA (Figure 5c). Using mass spectrometry we determined the D-peptide/U-peptide ratio of the peptide with N156 and N160, and we used the results for WC-gp120 as standard (Figure 5b). Similar to Figure 3c two histograms were plotted for this peptide (Figure 5b). The results showed that S158T mutation increased the glycosylation efficiency of N156 more than two-fold because the D-peptide/U-peptide ratio of S158T-H-CO-gp120 compared with that of H-CO-g120 increased more than two-fold in the histogram for the peptide with both N156 and N160 glycosylated (Figure 5b). T162S mutation decreased the glycosylation efficiency of N160 ca. two-fold because the D-peptide/U-peptide ratio of T162S-H-CO-gp120 compared with that of H-CO-gp120 in both histograms of Figure 5b decreased ca. two-fold. These changes were specific to N156 and N160 because calculation of the D-peptide/U-peptide ratio for the glycosylation site N461 did not show any difference among the constructs (Figure S5 in the Supporting Information). ELISA

dx.doi.org/10.1021/pr500740n | J. Proteome Res. 2014, 13, 5801−5811

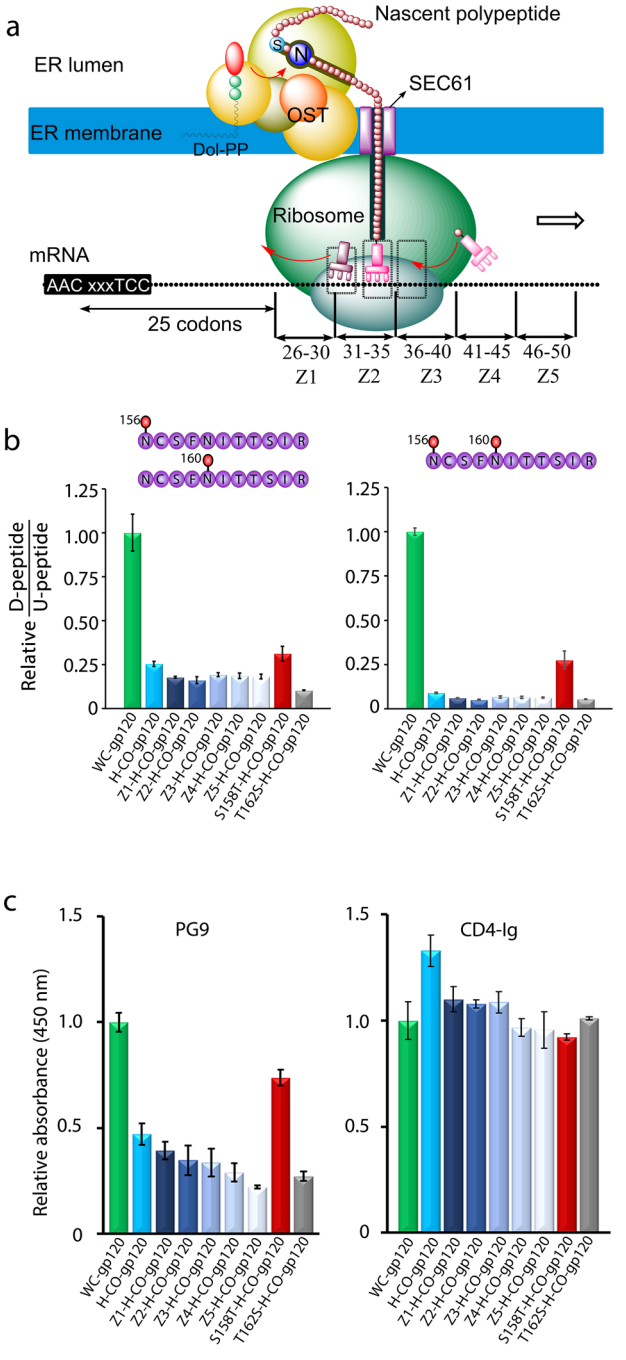

Figure 5. Effect of local synonymous codon change on the N-linked glycosylation efficiency and antibody binding. (a) Schematic presentation of the process that leads to the addition of N-linked oligosaccharides to a nascent polypeptide cotranslationally. The position is shown of the codons that are located downstream of the codons for a glycosylation motif and that were subjected to silent mutation in the gene encoding CO-gp120. (b) Effect of silent mutations downstream of the codon for N156 on the glycosylation efficiency of this site as measured by mass spectrometry. The results are compared with those obtained for the effect of S158T and T162S mutations on the N-lined glycosylation efficiency at positions N156 and N160, respectively. Two histograms are shown: a histogram for two peptides with either N156 or N160 glycosylated and a histogram for the peptide with both N156 and N160 glycosylated. The results are the average of two independent measurements ± plot ranges. One batch of protein was used. (c) Effect of silent mutations downstream of the N156 codon on PG9 and CD4-Ig binding as measured by ELISA. Concentration of gp120 was 2 mg/mL and those of PG9 and CD4-Ig were 10 mg/mL. The data for PG9 binding are corrected for small variations in concentration using the control experiment with CD4-Ig. The results are the average of two independent measurements ± standard deviation. Each experiment was performed in triplicate with two different batches of protein. All protein samples used in panels b and c were expressed and purified in parallel under identical conditions. One of the batches of protein that was used for ELISA experiments was used for mass spectrometry measurements.

experiments confirmed the results of mass spectrometry regarding two-fold increase in the glycosylation efficiency at N156 because of S158T mutation and two-fold decrease in the glycosylation efficiency at N160 due to T162S mutation (Figure 5c). However, mass spectrometry showed that changing five codons downstream of N156 and N160 did not significantly affect the frequency with which oligosaccharides were added to these positions (Figure 5b), whereas ELISA showed a reduction in PG9 binding (Figure 5c). This is opposite of what was expected: changing optimized codons to poor codons increases the glycosylation efficiency and PG9 binding. Whether changing more codons will have more effect on the N-linked glycosylation efficiency requires further investigation.

DISCUSSION

The effect of codon optimization, which is widely used to overcome poor expression of many viral proteins such as HIV-1 gp120,[2−7] on functional properties of viral glycoproteins has poorly been studied. We sought to test whether codon optimization changes the N-linked glycosylation efficiency of HIV-1 gp120. To this goal a new bottom-up mass spectrometry approach was applied to identify the peptides in which the asparagine residue of the NxS/T motif was glycosylated and could be deglycosylated by the PNGase F activity (D-peptide) and the peptides in which the asparagine residue was not glycosylated (U-peptide). Using this method we identified D- and U-peptides for all of the glycosylation sites that could be measured by trypsin digestion of gp120. For peptides with multiple glycosylation sites different D-peptides were observed depending on which sites were deglycosylated by the PNGase F activity. Among the peptides with multiple glycosylation sites we found a D-peptide in which three glycosylation sites were deglycosylated, namely, the peptide with glycosylation sites N136, N141, and N142. This observation appeared not to be due to background deamidation because the D-peptide/U-peptide ratio for this peptide (Table S2 in the Supporting Information) was much higher than the background level (Table 2). As a result deglycosylation of the NxS/T motifs by PNGase F and deamidation of N136, N141, and N142 must have led to the formation of this D-peptide. It is unlikely that two adjacent sites, that is, N141 and N142, were glycosylated by one catalytic subunit of OST because the addition of the oligosaccharide precursor to the first site will possibly interfere with addition of the oligosaccharide by the same complex to the next site. We suggest that N141 and N142 were both glycosylated by the activity of two different OST complexes that possibly one contains STT3A and the other contains STT3B as active subunits. This suggestion is based on the previous studies that show that STT3A and STT3B are two different catalytically active subunits of OST complex[17] and they appear to reside on different OST complexes[35] and on the

dx.doi.org/10.1021/pr500740n | J. Proteome Res. 2014, 13, 5801−5811

observation that the glycosylation of extremely close NxS/T motifs is dependent on the activity of STT3B subunit.[36]

After identification of D- and U-peptides, the mass spectrometry workflow in combination with ELISA was used to study the effect of codon optimization on the glycosylation efficiency of HIV-1 gp120 and on PG9 binding to gp120. We compared the D-peptide/U-peptide ratios of the protein product of a gp120 gene whose codon was not optimized (WC-gp120) with that of the codon optimized gene (CO-gp120). For three different expression levels of CO-gp120 it was observed that CO-gp120 was less efficiently glycosylated compared with WC-gp120 (Figure 3). Because all protein samples were expressed and purified in parallel under identical conditions (Experimental Procedure), the difference in the glycosylation efficiency of WC-gp120 and CO-gp120 could not be due to a difference in protein expression or purification condition or in the efficiency with which lectin captured gp120. Because CO-gp120 is less efficiently glycosylated than WC-gp120, the amount of CO-gp120 that was lost during lectin purification was possibly higher than that of WC-gp120. Thus, the difference between the glycosylation efficiency of WC-gp120 and CO-gp120 might be even higher than what we observed by mass spectrometry. Besides, the difference between the glycosylation efficiency of WC-gp120 and CO-gp120 cannot be associated with the nutrition depletion during overexpression of CO-gp120 because of three reasons: (I) For the low expression of CO-gp120 (L-CO-gp120) the amount of purified protein (Table 1) and the overall glycosylation efficiency (Figure 3) were less than those of WC-gp120. If the difference between the glycosylation efficiency of WC-gp120 and CO-gp120 were due to nutrition depletion during protein expression, WC-gp120 should have been glycosylated less efficiently than L-CO-gp120. (II) A plot of the amount of purified CO-gp120 as a function of the amount of plasmid used to transfect cells (Figure S6a in the Supporting Information) showed that the amount of purified CO-gp120 increased linearly from low (L-CO-g120) to medium (M-CO-gp120). Because nutrition depletion will reduce protein expression level, we can conclude that nutrition depletion did not occur for the M-CO-gp120. Therefore, the difference between M-CO-gp120 and WC-gp120 (Figure 3) cannot also be associated with the nutrition depletion during expression of CO-gp120. (III) For high expression level of CO-gp120 (H-CO-gp120), the amount of purified protein did not increase linearly as a function of the amount of plasmid used for the transfection of cells (Figure S6a in the Supporting Information). Thus, for H-CO-gp120 either nutrition depletion occurred or the cellular machinery reached its maximum speed for expression of protein. A plot of the glycosylation efficiency for low, medium, and high expression of CO-gp120 as a function of the amount of CO-gp120 purified (Figure S6b in the Supporting Information) showed that it changed linearly as a function of purified protein. If nutrition depletion occurred for H-CO-gp120, it would have been expected that the glycosylation efficiency as a function of the amount of purified CO-gp120 did not change linearly. Thus, nutrition depletion did not cause the difference between the glycosylation efficiency of H-CO-gp120 and WC-gp120.

We conclude that codon optimization increased the overall rate of gp120 expression. Further investigation is required to understand exactly which step during expression of gp120 was affected: the rate of transcription of DNA that leads to different mRNA copy numbers, the rate of translation of individual mRNAs, or the rate of degradation of nonglycosylated or poorly glycosylated proteins by the endoplasmic reticulum degradation pathway. Reduction in the glycosylation efficiency due to an increase in the translation rate has been reported for the human tyrosinase.[37] The increase in overall rate of gp120 production possibly overwhelmed the N-linked glycosylation machinery and led to reduction in the glycosylation efficiency of the NxS/T motifs in CO-gp120 compared with those in WC-gp120. Moreover, the glycosylation efficiency of CO-gp120 at a low expression level (L-CO-gp120) was less than that of WC-gp120 (Figure 3b). Therefore, poor codons might also affect the glycosylation efficiency by other mechanisms than increasing the overall translation rate. We propose that the presence of poor codons, that is, codons that are poorly used by the human genome, in the HIV-1 gp120 gene tunes the overall gp120 expression rate and assures its efficient glycosylation, which is essential for protein function and HIV-1 escape from the immune system.[8] This conclusion is in line with the observation that CO-gp120 has higher in vivo expression level, leading to higher antibody titers and cytotoxic T-lymphocyte reactivity.[38] We suggest that the increase in the immune response to the in vivo expression of codon-optimized gp120 (CO-gp120)[38,39] is at least partially due to less efficient glycosylation of this protein, which results in an impaired glycan shield and stimulation of the immune response.

To identify a possible mechanism by which poor codons might have affected glycosylation efficiency, we tested the effect of these codons downstream of the glycosylation sites N156 and N160 on the glycosylation efficiency and PG9 binding. Mass spectrometry and ELISA showed that PG9 binds to both oligosaccharides at positions N156 and N160. These results are in agreement with previous studies, which demonstrated that PG9 binding to gp120 is sensitive to the oligosaccharides at positions N156 and N160.[13,28] Mass spectrometry showed that changing five codons downstream of the glycosylation site N156 in CO-gp120 did not change the efficiency of glycosylation at N156 or N160, while PG9 binding was reduced as measured by ELISA. The reason for this observation is not known. Several studies have shown that codon usage may affect translation rate and folding of proteins in *E. coli*.[40−42] Therefore, it is possible that changing the codons downstream of N156, for example, codon 46 to codon 50 in Z5-H-CO-gp120 (Figure 5c), affected the local folding of an epitope in gp120 that is recognized by PG9 and thus affected PG9 binding, as measured by ELISA. This interpretation is in agreement with the finding that PG9 recognizes a structural epitope near the N156 glycosylation site in the V2 loop of HIV-1 gp120.[13] Further experiments are required to support this proposal.

In conclusion, we established a novel workflow for measuring site-specific N-linked glycosylation efficiency in glycoproteins. It was shown that codon optimization reduces the glycosylation efficiency of HIV-1 gp120 and affects binding of glycan dependent antibodies. Our mass spectrometry approach can further be applied in combination with isotope-labeling experiments to quantitatively determine the glycosylation efficiency of the NxS/T sequences of HIV-1 gp120 or other glycoproteins. This approach also provides the possibility to study the importance of N-linked oligosaccharides on bNABs binding. It is well known that mutation of serine in the NxS sequence to threonine increases the glycosylation efficiently of the asparagine residue;[9,17,43] therefore, by mutating T → S or S → T in the NxS/T motifs and applying our workflow to measure the decrease or increase in the glycosylation efficiency,

dx.doi.org/10.1021/pr500740n | J. Proteome Res. 2014, 13, 5801−5811

it will be feasible to directly observe the dependency of bNABs binding on specific glycosylation sites. Currently, these studies are performed using site-directed mutagenesis to replace asparagine in the NxS/T motif with alanine.[44,45] Replacement of an asparagine residue with an alanine may significantly affect local folding of the epitope that is recognized by bNABs and thus their binding. Our method cannot be applied to study N-linked glycosylation efficiency when the N-linked oligosaccharides have an α1−3 fucose on the innermost GlcNAc residue because in this case PNGase will not be able to cleave the oligosaccharide and deamidate the asparagine residue.[46] α1−3 focuse modification on the innermost GlcNAc residue is common among plants and some insects.[47]

■ ASSOCIATED CONTENT

Supporting Information

Table S1. List of peptides that were identified from MS/MS data. Table S2. The D-peptide/U-peptide ratio of the peptides with one or more NxS/T motifs. Table S3. List of peptides that were observed because of autodeamidation of asparagine residues outside the NxS/T motif. Figure S1. SDS gel showing that lectin could efficiently bind and release gp120. Figure S2. MS spectrum of NCSFDITTSIR peptide. Figure S3. MS/MS spectra of a D-peptide and its corresponding U-peptide. Figure S4. Schematic representation of the proteomic sequence coverage for gp120. Figure S5. Changing the codons downstream of glycosylation N156 does not affect other glycosylation sites. Figure S6. Nutrition depletion does not occur and does not affect glycosylation efficiency. Supplementary text. gp120 amino acid sequence library. This material is available free of charge via the Internet at http://pubs.acs.org.

■ AUTHOR INFORMATION

Corresponding Author

*Tel: +31 15 278 2347. E-mail: k.h.ebrahimi@tudelft.nl.

Present Address

‖G.M.W.: Biological Mass Spectrometry, Structural Biology & Biophysics, Pfizer Pharma Therapeutics Research & Development, Eastern Point Road, Groton, CT 06340.

Notes

The authors declare no competing financial interest.

■ ACKNOWLEDGMENTS

We thank professor Michael Farzan (The Scripps Research Institute) for his support during this research. Dr. Brian Quinlan (The Scripps Research Institute) is acknowledged for providing the constructs for expression of WC-gp120 and CO-gp120. We thank professor W. R. Hagen (Delft University of Technology) for his support. This research was financially supported by National Institutes of Health (NIH), USA, and Delft University of Technology.

■ REFERENCES

(1) Haas, J.; Park, E.-C.; Seed, B. Codon usage limitation in the expression of HIV-1 envelope glycoprotein. *Curr. Biol.* **1996**, *6*, 315.

(2) Go, E. P.; Irungu, J.; Zhang, Y.; Dalpathado, D. S.; Liao, H.-X.; Sutherland, L. L.; Alam, S. M.; Haynes, B. F.; Desaire, H. Glycosylation Site-Specific Analysis of HIV Envelope Proteins (JR-FL and CON-S) Reveals Major Differences in Glycosylation Site Occupancy, Glycoform Profiles, and Antigenic Epitopes' Accessibility. *J. Proteome Res.* **2008**, *7*, 1660.

(3) Go, E. P.; Liao, H.-X.; Alam, S. M.; Hua, D.; Haynes, B. F.; Desaire, H. Characterization of Host-Cell Line Specific Glycosylation Profiles of Early Transmitted/Founder HIV-1 gp120 Envelope Proteins. *J. Proteome Res.* **2013**, *12*, 1223.

(4) Spearman, P.; Lally, M. A.; Elizaga, M.; Montefiori, D.; Tomaras, G. D.; McElrath, M. J.; Hural, J.; De Rosa, S. C.; Sato, A.; Huang, Y.; Frey, S. E.; Sato, P.; Donnelly, J.; Barnett, S.; Corey, L. J.; NIAID, t. H. V. T. N. o. A Trimeric, V2-Deleted HIV-1 Envelope Glycoprotein Vaccine Elicits Potent Neutralizing Antibodies but Limited Breadth of Neutralization in Human Volunteers. *J. Infect. Dis.* **2011**, *203*, 1165.

(5) Zolla-Pazner, S.; deCamp, A.; Gilbert, P. B.; Williams, C.; Yates, N. L.; Williams, W. T.; Howington, R.; Fong, Y.; Morris, D. E.; Soderberg, K. A.; Irene, C.; Reichman, C.; Pinter, A.; Parks, R.; Pitisuttithum, P.; Kaewkungwal, J.; Rerks-Ngarm, S.; Nitayaphan, S.; Andrews, C.; O'Connell, R. J.; Yang, Z.-y.; Nabel, G. J.; Kim, J. H.; Michael, N. L.; Montefiori, D. C.; Liao, H.-X.; Haynes, B. F.; Tomaras, G. D. Vaccine-Induced IgG Antibodies to V1V2 Regions of Multiple HIV-1 Subtypes Correlate with Decreased Risk of HIV-1 Infection. *PLoS One* **2014**, *9*, e87572.

(6) Liu, F.; Mboudjeka, I.; Shen, S.; Chou, T.-H. W.; Wang, S.; Ross, T. M.; Lu, S. Independent but not synergistic enhancement to the immunogenicity of DNA vaccine expressing HIV-1 gp120 glycoprotein by codon optimization and C3d fusion in a mouse model. *Vaccine* **2004**, *22*, 1764.

(7) Gao, F.; Li, Y.; Decker, J. M.; Peyerl, F. W.; Bibollet-Ruche, F.; Rodenburg, C. M.; Chen, Y.; Shaw, D. R.; Allen, S.; Musonda, R.; Shaw, G. M.; Zajac, A. J.; Letvin, N.; Hahn, B. H. Codon usage optimization of HIV type 1 subtype C gag, pol, env, and nef genes: in vitro expression and immune responses in DNA-vaccinated mice. *AIDS Res. Hum. Retroviruses* **2003**, *19*, 817.

(8) Wei, X.; Decker, J. M.; Wang, S.; Hui, H.; Kappes, J. C.; Wu, X.; Salazar-Gonzalez, J. F.; Salazar, M. G.; Kilby, J. M.; Saag, M. S. Antibody neutralization and escape by HIV-1. *Nature* **2003**, *422*, 307.

(9) Chen, M. M.; Glover, K. J.; Imperiali, B. From peptide to protein: comparative analysis of the substrate specificity of N-linked glycosylation in C. jejuni. *Biochemistry* **2007**, *46*, 5579.

(10) Shakin-Eshleman, S. H.; Spitalnik, S. L.; Kasturi, L. The amino acid at the X position of an Asn-X-Ser sequon is an important determinant of N-linked core-glycosylation efficiency. *J. Biol. Chem.* **1996**, *271*, 6363.

(11) Mellquist, J.; Kasturi, L.; Spitalnik, S.; Shakin-Eshleman, S. The amino acid following an asn-X-Ser/Thr sequon is an important determinant of N-linked core glycosylation efficiency. *Biochemistry* **1998**, *37*, 6833.

(12) McLellan, J. S.; Pancera, M.; Carrico, C.; Gorman, J.; Julien, J.-P.; Khayat, R.; Louder, R.; Pejchal, R.; Sastry, M.; Dai, K. Structure of HIV-1 gp120 V1/V2 domain with broadly neutralizing antibody PG9. *Nature* **2011**, *480*, 336.

(13) Doores, K. J.; Burton, D. R. Variable loop glycan dependency of the broad and potent HIV-1-neutralizing antibodies PG9 and PG16. *J. Virol.* **2010**, *84*, 10510.

(14) Walker, L. M.; Huber, M.; Doores, K. J.; Falkowska, E.; Pejchal, R.; Julien, J.-P.; Wang, S.-K.; Ramos, A.; Chan-Hui, P.-Y.; Moyle, M. Broad neutralization coverage of HIV by multiple highly potent antibodies. *Nature* **2011**, *477*, 466.

(15) Tarentino, A. L.; Gomez, C. M.; Plummer, T. H., Jr. Deglycosylation of asparagine-linked glycans by peptide: N-glycosidase F. *Biochemistry* **1985**, *24*, 4665.

(16) Mohorko, E.; Glockshuber, R.; Aebi, M. Oligosaccharyltransferase: the central enzyme of N-linked protein glycosylation. *J. Inherited Metab. Dis.* **2011**, *34*, 869.

(17) Aebi, M. N-linked protein glycosylation in the ER. *BBA, Biochim. Biophys. Acta, Mol. Cell Res.* **2013**, *1833*, 2430.

(18) Robinson, A. B.; McKerrow, J. H.; Cary, P. Controlled deamidation of peptides and proteins: an experimental hazard and a possible biological timer. *Proc. Natl. Acad. Sci. U.S.A.* **1970**, *66*, 753.

(19) Zhu, X.; Borchers, C.; Bienstock, R. J.; Tomer, K. B. Mass spectrometric characterization of the glycosylation pattern of HIV-gp120 expressed in CHO cells. *Biochemistry* **2000**, *39*, 11194.

(20) Balzarini, J.; Van Laethem, K.; Hatse, S.; Froeyen, M.; Van Damme, E.; Bolmstedt, A.; Peumans, W.; De Clercq, E.; Schols, D. Marked depletion of glycosylation sites in HIV-1 gp120 under selection pressure by the mannose-specific plant lectins of Hippeastrum hybrid and Galanthus nivalis. *Mol. Pharm.* **2005**, *67*, 1556.
(21) Maley, F.; Trimble, R. B.; Tarentino, A. L.; Plummer, T. H., Jr. Characterization of glycoproteins and their associated oligosaccharides through the use of endoglycosidases. *Anal. Biochem.* **1989**, *180*, 195.
(22) Katiyar, S.; Suzuki, T.; Balgobin, B. J.; Lennarz, W. J. Site-directed mutagenesis study of yeast peptide: N-glycanase Insight into the reaction mechanism of deglycosylation. *J. Biol. Chem.* **2002**, *277*, 12953.
(23) Morelle, W.; Michalski, J.-C. Analysis of protein glycosylation by mass spectrometry. *Nat. Protoc.* **2007**, *2*, 1585.
(24) Lundby, A.; Olsen, J. V. GeLCMS for in-Depth Protein Characterization and Advanced Analysis of Proteomes. *Methods Mol. Biol.* **2011**, *753*, 143.
(25) Tyler-Cross, R.; Schirch, V. Effects of amino acid sequence, buffers, and ionic strength on the rate and mechanism of deamidation of asparagine residues in small peptides. *J. Biol. Chem.* **1991**, *266*, 22549.
(26) Wright, H. T. Sequence and structure determinants of the nonenzymatic deamidation of asparagine and glutamine residues in proteins. *Protein Eng.* **1991**, *4*, 283.
(27) Wright, H. T. Nonenzymatic deamidation of asparaginyl and glutaminyl residues in proteins. *Crit. Rev. Biochem. Mol. Biol.* **1990**, *26*, 1.
(28) Amin, M. N.; McLellan, J. S.; Huang, W.; Orwenyo, J.; Burton, D. R.; Koff, W. C.; Kwong, P. D.; Wang, L.-X. Synthetic glycopeptides reveal the glycan specificity of HIV-neutralizing antibodies. *Nat. Chem. Biol.* **2013**, *9*, 521.
(29) Julien, J.-P.; Lee, J. H.; Cupo, A.; Murin, C. D.; Derking, R.; Hoffenberg, S.; Caulfield, M. J.; King, C. R.; Marozsan, A. J.; Klasse, P. J. Asymmetric recognition of the HIV-1 trimer by broadly neutralizing antibody PG9. *Proc. Natl. Acad. Sci. U.S.A.* **2013**, *110*, 4351.
(30) Walker, L. M.; Phogat, S. K.; Chan-Hui, P.-Y.; Wagner, D.; Phung, P.; Goss, J. L.; Wrin, T.; Simek, M. D.; Fling, S.; Mitcham, J. L. Broad and potent neutralizing antibodies from an African donor reveal a new HIV-1 vaccine target. *Science* **2009**, *326*, 285.
(31) Davenport, T. M.; Friend, D.; Ellingson, K.; Xu, H.; Caldwell, Z.; Sellhorn, G.; Kraft, Z.; Strong, R. K.; Stamatatos, L. Binding interactions between soluble HIV envelope glycoproteins and quaternary-structure-specific monoclonal antibodies PG9 and PG16. *J. Virol.* **2011**, *85*, 7095.
(32) Euler, Z.; Bunnik, E. M.; Burger, J. A.; Boeser-Nunnink, B. D.; Grijsen, M. L.; Prins, J. M.; Schuitemaker, H. Activity of broadly neutralizing antibodies, including PG9, PG16, and VRC01, against recently transmitted subtype B HIV-1 variants from early and late in the epidemic. *J. Virol.* **2011**, *85*, 7236.
(33) Ménétret, J.-F.; Neuhof, A.; Morgan, D. G.; Plath, K.; Radermacher, M.; Rapoport, T. A.; Akey, C. W. The structure of ribosome-channel complexes engaged in protein translocation. *Mol. Cell* **2000**, *6*, 1219.
(34) Bause, E.; Legler, G. The role of the hydroxy amino acid in the triplet sequence Asn-Xaa-Thr (Ser) for the N-glycosylation step during glycoprotein biosynthesis. *Biochem. J.* **1981**, *195*, 639.
(35) Shrimal, S.; Ng, B. G.; Losfeld, M.-E.; Gilmore, R.; Freeze, H. H. Mutations in STT3A and STT3B cause two congenital disorders of glycosylation. *Hum. Mol. Genet.* **2013**, *22*, 4638.
(36) Shrimal, S.; Gilmore, R. Glycosylation of closely spaced acceptor sites in human glycoproteins. *J. Cell Sci.* **2013**, *126*, 5513.
(37) Újvári, A.; Aron, R.; Eisenhaure, T.; Cheng, E.; Parag, H. A.; Smicun, Y.; Halaban, R.; Hebert, D. N. Translation Rate of Human Tyrosinase Determines ItsN-Linked Glycosylation Level. *J. Biol. Chem.* **2001**, *276*, 5924.
(38) André, S.; Seed, B.; Eberle, J.; Schraut, W.; Bültmann, A.; Haas, J. Increased immune response elicited by DNA vaccination with a synthetic gp120 sequence with optimized codon usage. *J. Virol.* **1998**, *72*, 1497.
(39) Kutzler, M. A.; Weiner, D. B. DNA vaccines: ready for prime time? *Nat. Rev. Gen.* **2008**, *9*, 776.
(40) Komar, A. A.; Lesnik, T.; Reiss, C. Synonymous codon substitutions affect ribosome traffic and protein folding during in vitro translation. *FEBS Lett.* **1999**, *462*, 387.
(41) Orešič, M.; Shalloway, D. Specific correlations between relative synonymous codon usage and protein secondary structure. *J. Mol. Biol.* **1998**, *281*, 31.
(42) Cortazzo, P.; Cerveñansky, C.; Marín, M.; Reiss, C.; Ehrlich, R.; Deana, A. Silent mutations affect in vivo protein folding in *Escherichia coli*. *Biochem. Biophys. Res. Commun.* **2002**, *293*, 537.
(43) Kasturi, L.; Eshleman, J. R.; Wunner, W. H.; Shakin-Eshleman, S. H. The hydroxy amino acid in an Asn-X-Ser/Thr sequon can influence N-linked core glycosylation efficiency and the level of expression of a cell surface glycoprotein. *J. Biol. Chem.* **1995**, *270*, 14756.
(44) Kong, L.; Lee, J. H.; Doores, K. J.; Murin, C. D.; Julien, J.-P.; McBride, R.; Liu, Y.; Marozsan, A.; Cupo, A.; Klasse, P.-J. Supersite of immune vulnerability on the glycosylated face of HIV-1 envelope glycoprotein gp120. *Nat. Struct. Mol. Biol.* **2013**, *20*, 796.
(45) Falkowska, E.; Le, K. M.; Ramos, A.; Doores, K. J.; Lee, J. H.; Blattner, C.; Ramirez, A.; Derking, R.; van Gils, M. J.; Liang, C.-H. Broadly neutralizing HIV antibodies define a glycan-dependent epitope on the prefusion conformation of gp41 on cleaved envelope trimers. *Immunity* **2014**, *40*, 657.
(46) Tretter, V.; Altmann, F.; März, L. Peptide-N4-(N-acetyl-β-glucosaminyl) asparagine amidase F cannot release glycans with fucose attached α1→ 3 to the asparagine-linked N-acetylglucosamine residue. *Eur. J. Biochem.* **1991**, *199*, 647.
(47) Wilson, I. B. Glycosylation of proteins in plants and invertebrates. *Curr. Opin. Struct. Biol.* **2002**, *12*, 569.